Frequency shifts of the magnetic-resonance spectrum of mixtures of nuclear spin-polarized noble gases and vapors of spin-polarized alkali-metal atoms

S. R. Schaefer, G. D. Cates, Ting-Ray Chien, D. Gonatas, W. Happer, and T. G. Walker
Department of Physics, Princeton University, Princeton, New Jersey 08544
(Received 3 October 1988)

We report the first quantitative theoretical and experimental studies of frequency shifts of nuclear-magnetic-resonance (NMR) lines of noble-gas atoms and the corresponding frequency shifts of electron-paramagnetic-resonance (EPR) lines of alkali-metal atoms in mixtures of nuclear spin-polarized noble gases and vapors of spin-polarized alkali-metal atoms. The shifts are primarily due to the Fermi-contact hyperfine interaction. For the heavier noble gases there can be relatively large ($\approx 10\%$) contributions to the shifts from van der Waals molecules. The NMR frequencies of polarized ^{83}Kr and ^{129}Xe were measured in a vapor of spin-polarized alkali-metal atoms oriented parallel and antiparallel to the external magnetic field. The shift in the EPR frequency of the alkali-metal vapor due to the polarized noble-gas nuclei was measured simultaneously, thus providing a measurement of the absolute noble-gas nuclear polarization. The frequency shifts can be used as a convenient way to measure the absolute nuclear spin polarization of noble gases.

I. INTRODUCTION

Polarizing nuclear spins through spin exchange[1,2] with optically pumped alkali-metal vapors has become increasingly widespread. Applications have included precise measurements of magnetic moments,[3-5] searches for permanent electric dipole moments in atoms,[6] surface studies,[7,8] and polarized nuclear targets.[9] Magnetic resonance is often employed in these experiments, and when there is a need to determine magnetic-resonance frequencies precisely, it is important to identify mechanisms which can result in frequency shifts. As was first shown by Grover,[10] the spin-polarized nuclei of noble-gas atoms will cause a shift in the EPR frequency of the alkali-metal atoms when both types of atoms are in the same gaseous sample. Similarly, the spin-polarized valence electrons of alkali-metal atoms will cause a shift of the NMR frequency of noble gases. These shifts are due to the well-known Fermi-contact interaction $\alpha\mathbf{K}\cdot\mathbf{S}$ between the nuclear spin $\mathbf{K}$ of the noble-gas nucleus of magnetic moment μ_K and the electron spin $\mathbf{S}$ of the alkali atom. The coupling constant α depends on the distance R between the nuclei of the noble-gas and the alkali-metal atom, and can be written as

$$\alpha=\frac{8\pi}{3}g_S\mu_B\frac{\mu_K}{K}|\psi(R)|^2 . \tag{1}$$

Here $|\psi(R)|^2$ is the square of the valence-electron wave function of the alkali-metal atom at the site of the noble-gas nucleus, $g_S\approx 2$ is the Landé g factor, and μ_B is the Bohr magneton. The shift is closely analogous to the Knight shift,[11] caused by polarized conduction electrons, in the magnetic-resonance frequency of nuclei in metals, and to the pressure shift[12] of alkali-metal-vapor frequency standards, both of which are due to the interaction (1).

We have made a quantitative experimental study of frequency shifts in the ^{83}KrRb and ^{129}XeRb systems. These shifts are by no means small. For example, in Fig. 1 we show two NMR lines, corresponding to the ground-state Zeeman splitting in ^{83}Kr. The NMR lines were measured in the presence of polarized alkali-metal vapor. The curves correspond to alkali-metal spins oriented parallel and antiparallel to the external magnetic field. The details of the experiment are described in Sec. III.

At low magnetic fields where the quadratic Zeeman splitting of the alkali-metal EPR resonance frequencies is negligible, the EPR frequency shift due to the polarized noble-gas atoms is

$$\Delta|\nu_A|=\frac{1}{h}\frac{\mu_B|g_S|}{(2I+1)}\frac{8\pi}{3}\frac{\mu_K}{K}\kappa_{AX}[X]\langle K_z\rangle . \tag{2}$$

The NMR frequency shift of the noble-gas atoms due to the polarized alkali-metal vapor is given by the analogous formula

$$\Delta|\nu_X|=-\frac{1}{h}\frac{|\mu_K|}{K}\frac{8\pi}{3}\mu_B g_S\kappa_{XA}[A]\langle S_z\rangle . \tag{3}$$

Here $[X]$ is the noble-gas density, $[A]$ is the number density of alkali-metal atoms, I is the spin of the alkali-metal nucleus, $\langle K_z\rangle$ is the longitudinal spin of the noble-gas nuclei, $\langle S_z\rangle$ is the longitudinal spin of the alkali-metal valence electrons and h is Planck's constant. The dimensionless *enhancement factors* κ_{AX} and κ_{XA} were introduced by Grover[10] to describe the frequency shifts which he observed in spin-polarized mixtures of rubidium vapor and the noble-gas isotopes ^{83}Kr and ^{129}Xe. Grover defined κ_{AX} as the ratio of the mean magnetic field increment, actually experienced by the valence electrons of the alkali-metal atoms, to the macroscopic field increment $(8\pi/3)(\mu_K/K)\langle K_z\rangle[X]$ which would be produced in a spherical cell by a noble gas with the same density and nuclear-spin polarization. The enhancement factor κ_{XA} has an analogous meaning.

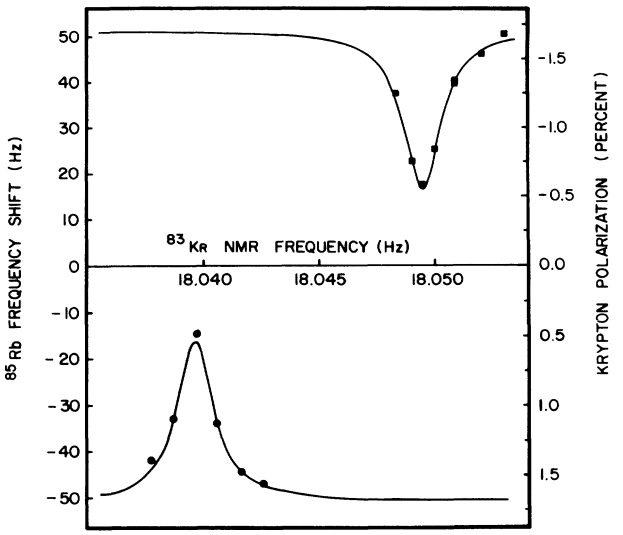

FIG. 1. Nuclear-magnetic-resonance (NMR) scan for ^{83}Kr. For the lower resonance curve, $\langle S_z \rangle$ and $\langle K_z \rangle$ are parallel to the external magnetic field B; and for the upper curve, $\langle S_z \rangle$ and $\langle K_z \rangle$ are antiparallel to the external field. The nuclear resonance appears as a decrease in the magnitude of the electron-paramagnetic-resonance (EPR) frequency shift. As discussed in the text, the EPR frequency shift is directly proportional to the nuclear spin polarization of the Kr atoms. The krypton polarization scale is subject to the 33% uncertainty in the Rb polarization. The width of the curves is dominated by the small splitting of the ^{83}Kr spin sublevels by the interaction of the nuclear quadrupole moment with an electric field gradient, which acts on the nucleus while the Kr atom is close to the surface of the sample cell.

In Sec. II B we show that it is possible to write the enhancement factors in the form

$$\kappa_{AX}=(\kappa_0-\kappa_1)+\epsilon_{AX}\kappa_1 \tag{4}$$

and

$$\kappa_{XA}=(\kappa_0-\kappa_1)+\epsilon_{XA}\kappa_1 \ . \tag{5}$$

Here $\kappa_0-\kappa_1$ is the contribution from free noble-gas–alkali-metal pairs and $\epsilon_{AX}\kappa_1$ and $\epsilon_{XA}\kappa_1$ are the contributions from bound pairs or van der Waals molecules.

Theoretical formulas for the parameters κ_0 and κ_1 are given by (18) and (28), respectively. However, κ_0 and κ_1 also have a simple physical interpretation, which we summarize here. Define $(|\psi|^2)_{\rm av}$, the ensemble-averaged valence-electron density at the nucleus of a noble-gas atom, as the sum of the valence-electron densities $|\psi|^2$ at each noble-gas nucleus in the sample at some instant of time, divided by the total number of noble-gas atoms in the sample. The valence-electron density at most nuclei will be nearly zero because there will be no alkali-metal atom close by. However, a small fraction of nuclei will be in the process of a binary collision with an alkali-metal atom, and for these nuclei $|\psi|^2$ will be relatively large. There will also be a small fraction of nuclei which are bound in van der Waals molecules, and $|\psi|^2$ will be relatively large for these nuclei too. Of course, the average valence-electron density $(|\psi|^2)_{\rm av}$ will be proportional to the number density $[A]$ of alkali-metal atoms, and the constant of proportionality is the enhancement factor κ_0, that is,

$$(|\psi|^2)_{\rm av}=\kappa_0[A] \ . \tag{6}$$

Similarly, we may define the contribution $(|\psi|_B^2)_{\rm av}$ to (6) from van der Waals molecules by adding the valence-electron densities $|\psi|^2$ at all noble-gas nuclei of van der Waals molecules, and dividing the sum by the total number of noble-gas atoms in the sample. The contribution $(|\psi|_B^2)_{\rm av}$ from van der Waals molecules will also be proportional to the number density $[A]$ of alkali-metal atoms, and the constant of proportionality is the enhancement factor κ_1, that is,

$$(|\psi|_B^2)_{\rm av}=\kappa_1[A] \ . \tag{7}$$

There is also a simple physical interpretation of the suppression factors ϵ_{AX} and ϵ_{XA}. When a van der Waals molecule is formed the electron spin **S** and the nuclear spin **I** of the alkali-metal atom will begin to precess about the rotational angular momentum **N** of the van der Waals molecule and about the nuclear spin **K** of the noble gas. If the molecule is quickly broken up again, neither $\langle K_z \rangle$ nor $\langle S_z \rangle$ will have had time to change very much from their values before the molecule was formed. However, if the molecule lives long enough, there will be large rotations of the angular momenta about each other. Consequently, the effective magnitudes of $\langle K_z \rangle$ and $\langle S_z \rangle$ which act within the molecule will be reduced by the suppression factors ϵ_{AX} and ϵ_{XA} to the values $\epsilon_{AX}\langle K_z \rangle$ and $\epsilon_{XA}\langle S_z \rangle$, respectively.

We show in Sec. II B that the suppression factors can be adequately represented by the formulas

$$\epsilon_{AX}=\frac{1+\frac{1}{3}(\phi/[I])^2}{[1+(\phi/[I])^2]^2} \ , \tag{8}$$

and

$$\epsilon_{XA}=\frac{2}{3}\frac{1}{1+(\phi/[I])^2}+\frac{1}{I(I+1)[I]}\sum_{m_I=-I}^{I}\frac{(m_I)^2}{1+(\phi m_I/x[I])^2} \ . \tag{9}$$

Statistical weights of angular momentum quantum numbers are denoted by square brackets, i.e.,

$$[I]=2I+1 \tag{10}$$

and m_I is one of the azimuthal quantum numbers of the alkali-metal nuclear spin. The phase angle is

$$\phi=\frac{\gamma N\tau}{\hbar} \ , \tag{11}$$

the product of the mean spin-rotation coupling frequency $\gamma N/\hbar$ and the mean lifetime τ of the van der Waals molecules. The Breit-Rabi parameter is

$$x=\frac{\gamma N}{\alpha} \ . \tag{12}$$

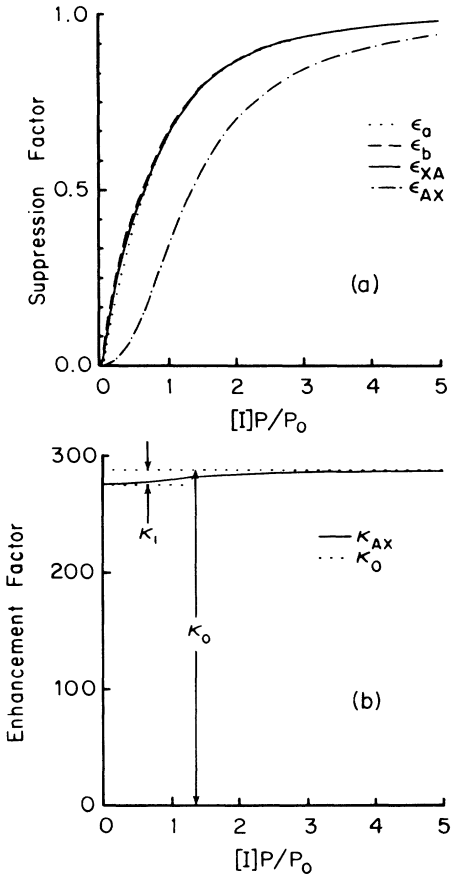

FIG. 2. (a) Frequency-shift suppression factors ϵ for van der Waals molecules. (b) Frequency-shift enhancement factor κ_{AX} (solid line) as a function of gas pressure for ^{83}Kr. At low pressures, the suppression of the van der Waals molecular contribution to the frequency shift reduces the value of κ_{AX} slightly from the high-pressure value κ_0 given by the upper dotted line.

To ensure the validity of the perturbative theory of Ref. 1, which was used to derive the suppression factors (8) and (9), it is necessary to have $x^2 \gg 1$.

The mean lifetime τ of the van der Waals molecules is inversely proportional to the gas pressure p in the cell and we can therefore write (11) as

$$\phi = \frac{p_0}{p} , \tag{13}$$

where p_0 is a characteristic pressure which depends on the composition of the sample gas. For example,[13] in the ^{129}Xe Cs system, if the gas is predominantly N_2, the ^{129}Xe Cs van der Waals molecules are almost always broken up in collisions with N_2 molecules and the characteristic pressure is $p_0 = 177$ torr. If the gas is predominantly He, the characteristic pressure is $p_0 = 384$ torr. Representative suppression factors ϵ_{XA} and ϵ_{AX} are shown in Fig. 2(a) as a function of the relative pressure p/p_0.

Values of the enhancement factors κ_0 and κ_1, as calculated with (18) and (28) at a temperature of 100 °C, are shown in Tables I and II. The temperature coefficients

TABLE I. Calculated values of the enhancement factors κ_0 from Eq. (18).

Alkali metal	He	Ne	Ar	Kr	Xe	Rn
Na	1.9	10.5	28.9	117	309	733
K	2.7	13.4	55.7	235	661	1340
Rb	2.7	15.0	60.5	276	726	1440
Cs	3.1	17.4	82.9	337	879	1820

T_0 of Table III were calculated according to (21), and they can be used in (22) to estimate values of κ_0 at temperatures other than the reference temperature $T_r = 100$ °C. Over the temperature range from 0 °C to 200 °C, the enhancement factor κ_1 is very nearly proportional to $T^{-3/2}$, where T is the absolute temperature.

The calculated values of κ_0 and κ_1 in Tables I and II are sensitive to two rather poorly known factors: the repulsive part of the van der Waals potential V and the wave-function enhancement factor η, first introduced by Herman[14] and defined in Eq. (15). As described below, we have used the most reliable values of V and η that are known to us to compute the numbers for Tables I and II. Precise measurements of the frequency shifts will provide useful constraints which can lead to more reliable experimental estimates of V and η. For the few cases where experimental measurements of κ_0 and κ_1 are available, the calculated values in Tables I and II are within about 10% of the measured values, so we think that the numbers in Tables I and II can be used as reasonable initial estimates of the true values of the enhancement factors.

As discussed in detail in Sec. III we have measured κ_0 for RbKr and RbXe. The measurements are summarized in Table IV along with the corresponding theoretical values from Table I. The theoretical estimates of κ_0 are within the estimated experimental error. The theoretical ratio $(\kappa_0)_{XeRb}/(\kappa_0)_{KrRb} = 2.63$ inferred from Table I, is in reasonable agreement with the experimentally determined ratio $(\kappa_0)_{XeRb}/(\kappa_0)_{KrRb} = 2.38 \pm 0.13$, which is discussed Sec. III.

So far there are no direct experimental measurements of the pressure dependence of the frequency shifts, which would allow one to judge the reliability of the theoretical estimates κ_1 in Table II. We can, however, estimate κ_1 indirectly from other experimentally measured quantities, as discussed in Sec. III. The results of these indirect estimates of κ_1 are summarized in Table IV, and are compared with the theoretical estimates of Tables I and II. The agreement between experimental and theoretical values of κ_1 is remarkably, and perhaps fortuitously, good.

Table II and Fig. 2 show that under most experimental conditions the van der Waals molecules, which are responsible for most of the spin-exchange and spin-relaxation *rates* for the heavier noble gases, contribute very little to the frequency *shifts*. In the most extreme case of Rn, the molecular contribution κ_1 is about 15% of κ_0 at 100 °C. Since the magnitude of κ_1 decreases more rapidly with temperature than the magnitude of κ_0, the contribution of molecules to the frequency shift will be-

TABLE II. Calculated values of the ratio κ_1/κ_0 at $T=100\,^{\circ}\mathrm{C}$ from Eqs. (18) and (28).

Alkali metal	He	Ne	Ar	Kr	Xe	Rn
Na	2.6×10^{-5}	6.9×10^{-4}	0.016	0.039	0.074	0.13
K	8.9×10^{-6}	6.6×10^{-4}	0.015	0.040	0.083	0.14
Rb	7.9×10^{-6}	7.1×10^{-4}	0.012	0.043	0.078	0.14
Cs	4.9×10^{-6}	8.2×10^{-4}	0.018	0.044	0.086	0.15

come less important as the temperature increases. At the pressures of many experiments, the contribution of the molecules to the frequency shift will be very nearly saturated (see Fig. 2), and will be nearly independent of small changes in the pressure.

The EPR frequency shift (2) is proportional to the noble-gas polarization. The insensitivity of the factor κ_{AX} to the pressure and temperature of the cell and the precision with which the frequency shift can be measured suggest that the EPR frequency shift could provide a convenient and precise new way to measure the nuclear-spin polarization of the optically pumped noble-gas targets which Chupp *et al.*[9] have developed for nuclear scattering experiments. The size of the expected shift is quite large. For instance, if 3.5 atmospheres of ^{3}He were 50% polarized, the shift would be about 5 kHz. Since frequencies can be determined very precisely, the precision of the polarization measurements would be limited only by the determination of κ_0, a quantity which in principle can be determined quite accurately by experiment, although probably not very accurately by calculation. When conventional NMR is used for the determination of an absolute polarization in an optically pumped target, the fractional error is typically inversely proportional to the size of the static magnetic holding field. In the case of Chupp's work, the magnetic field was between 30 and 100 G. At higher fields, nuclear polarizations are more easily determined, and a simultaneous measurement of the nuclear polarization using conventional NMR techniques and the EPR frequency shift could provide a measurement of κ_0 accurate to several percent. Such a measurement would provide a calibration for the interpretation of frequency shifts at lower fields, where polarimetry would otherwise be more difficult. Because of the low magnetic fields used in our measurements (≈ 0.11 G) conventional NMR techniques were impractical. Our measurements of κ_0 were thus limited by sensitivity to alkali-metal polarization and to alkali-metal number density.

The EPR frequency shift (2) due to the contact interaction (1) is independent of the cell shape, in contrast to the smaller shift due to the long-range magnetic dipole-dipole interaction, which depends on the shape of the sample through the classical *depolarization factor*.[15] In the case of the heavier nobles, the large value of the enhancement factor κ_0 ensures that the frequency shifts are independent of cell shape to better than 1%. In the case of the lighter nobles, such as He, Ne, and to some extent Ar, the enhancement factors are smaller, and care needs to be taken in accounting for some cell shape dependence due to the dipole-dipole interaction.

TABLE III. Calculated values of the temperature coefficient T_0 in °C at $T_r=100\,^{\circ}\mathrm{C}$ from (21). This Table may be used with Eq. (22) to calculate the temperature dependence of κ_0.

Alkali metal	He	Ne	Ar	Kr	Xe	Rn
Na	443	614	890	1220	2060	25 800
K	426	714	956	1430	3490	−5880
Rb	440	748	926	1700	3450	−4870
Cs	427	808	1270	2060	6380	−3560

II. BASIC THEORY OF THE FREQUENCY SHIFT

The simplest spin interaction Hamiltonian which is consistent with all data for alkali-metal noble-gas systems is[1]

$$H = A\mathbf{I}\cdot\mathbf{S}+\gamma\mathbf{N}\cdot\mathbf{S}+\alpha\mathbf{K}\cdot\mathbf{S} +g_S\mu_B\mathbf{B}\cdot\mathbf{S}-\frac{\mu_K}{K}\mathbf{B}\cdot\mathbf{K}+\cdots , \tag{14}$$

where $A\mathbf{I}\cdot\mathbf{S}$ is the hyperfine coupling between the electron spin $\mathbf{S}$ and the alkali-metal nuclear spin $\mathbf{I}$ and $\gamma\mathbf{N}\cdot\mathbf{S}$ is the coupling between the rotational angular momentum $\mathbf{N}$ of the alkali-metal–noble-gas pair and the electron spin of the alkali-metal atom. The term $\alpha\mathbf{K}\cdot\mathbf{S}$ is the Fermi-contact hyperfine interaction discussed in conjunction with Eq. (1). Herman[14] has pointed out that $\psi(R)$ is substantially larger than $\psi_0(R)$, the valence-electron wave function of the unperturbed ground-state alkali-metal atom at a distance R from the nucleus. Following Herman[14] we will define an enhancement factor for the wave function

$$\eta=\frac{\psi(R)}{\psi_0(R)} , \tag{15}$$

TABLE IV. Comparison of experimental results to theory. The values for κ_0 are from this work; the values of κ_1 are deduced from experiments of van der Waals molecules as discussed in the text. All theoretical numbers are at 100 °C. The measurement of κ_0 for RbKr was done at 90 °C, and we note that the expected correction due to the temperature difference is less than 1%. The measurement of the ratio of κ_0 for RbKr to κ_0 for RbXe, which was used to deduce the quoted value of κ_0 for RbXe, was done at 80 °C, and again the correction due to the temperature difference is expected to be less than 1%.

Pair	$(\kappa_0)_{\mathrm{expt}}$	$(\kappa_0)_{\mathrm{theor}}$	$(\kappa_1)_{\mathrm{expt}}$	$(\kappa_1)_{\mathrm{theor}}$
RbKr	270±95	276	11.7±2.5	11.9
RbXe	644±260	726	43.5±7.3	56.7
KXe		661	52.6±14.4	54.9
CsXe		879	58.9±22.1	75.5

and we will assume that η is independent of R and, for a given type of noble gas, is approximately the same for all alkali-metal atoms. Calculations of η have been carried out by Walker *et al.*[16] The last two terms in (14) are the interaction between an external magnetic field **B** and the spins **S** and **K**.

Since the measured frequency shift involves an average over many bound and free quantum states of the van der Waals molecules we shall approximate the averages with the methods of classical statistical mechanics. From the viewpoint of a single noble-gas atom the interaction (14) will be time dependent because the distance R will change during collisions. The coupling constants α and γ will be zero most of the time because no alkali-metal atom is nearby but they will become large for a few picoseconds during binary collisions, which occur every few milliseconds under representative experimental conditions (saturated Rb vapor at 90 °C). The duration of the binary collision is short enough that the spins precess only a tiny amount, typically 10^{-4} rad, during the collision. At much less frequent intervals, typically once a minute, the noble-gas atom forms a bound van der Waals molecule in a three-body collision for which a nitrogen molecule or another noble-gas atom is the third body. The interaction (14) can then act throughout the relatively long molecular lifetime τ of the van der Waals molecule and the spins **S** and **K** can rotate by large angles about each other and about the rotational angular momentum **N**. A representative collisionally limited molecular lifetime τ at a gas pressure of 35 torr is 2 ns.

Using the methods outlined in Ref. 1 one can show that the average value of the fluctuating microscopic interaction (14) produces a shift in the EPR frequencies of the alkali-metal atoms. The EPR shift can be ascribed to an effective static field acting on the alkali-metal valence electron

$$\delta \mathbf{B}_A = \frac{8\pi}{3}\frac{\mu_K}{K}\kappa_{AX}[X]\langle \mathbf{K}\rangle \ . \tag{16}$$

Similarly, there will be a shift in the noble-gas NMR frequency, which can be described by an effective field

$$\delta \mathbf{B}_X = -\frac{8\pi}{3} g_S \mu_B \kappa_{XA}[A]\langle \mathbf{S}\rangle \ . \tag{17}$$

The frequency shifts (2) and (3) follow from the effective magnetic fields (16) and (17), respectively.

A. Frequency shifts at high pressures

At high third-body pressures, where the spin-evolution angles during a molecular lifetime are small, it is possible to replace the time average of (14) by an ensemble average over a Boltzmann distribution of the rotational angular momentum **N** and of the internuclear separations R between the noble-gas and alkali-metal atoms. Then the effective magnetic fields $\delta \mathbf{B}_X$ and $\delta \mathbf{B}_A$ are the ensemble-averaged values of the term $\alpha \mathbf{K}\cdot\mathbf{S}$ of (14) per alkali-metal atom and per noble-gas atom, respectively. In this high-pressure limit the enhancement factors approach a common limiting value, $\kappa_{AX} \to \kappa_0$ and $\kappa_{XA} \to \kappa_0$, where

$$\kappa_0 = \eta^2 \int_0^\infty |\psi_0(R)|^2 e^{-V(R)/kT} 4\pi R^2 dR \ , \tag{18}$$

where $V(R)$ is the van der Waals potential which describes the force between an alkali-metal atom and a noble-gas atom.

Representative values of the van der Waals potential $V(R)$ and of the Boltzmann factor $e^{-V(R)/kT}$ for RbKr at 100 °C are shown in Fig. 3. Note that the well depth is about 30% of the thermal energy kT, so the Boltzmann factor does not greatly exceed unity, even at the minimum of the potential well. The parameters of the van der Waals potentials are determined from atomic scattering experiments and are subject to some ambiguities of interpretation.

We have used our best estimates of the van der Waals potentials V and wave-function enhancement factors η to calculate values of κ_0 at 100 °C according to (18). The potential curves used for Ar, Kr, and Xe are those of Pascale and Vandeplanque.[17] For He, the calculations of

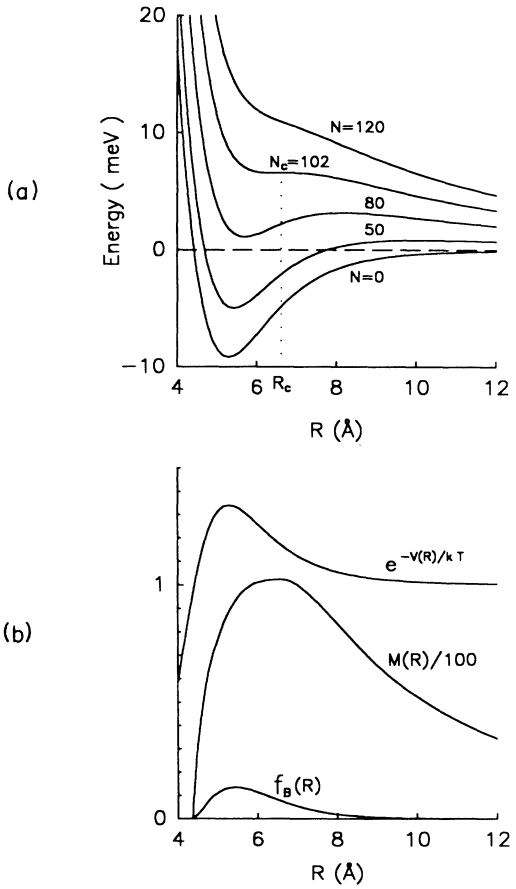

FIG. 3. Some representative properties of the RbKr van der Waals molecule. (a) Effective potential of Eq. (39) for various values of the rotational angular momentum N. The maximum angular momentum for which a bound RbKr can exist is $N_c \approx 102$. (b) Boltzmann factor occurring in Eq. (18), the maximum angular momentum $M(R)$ that a bound molecule can have at an internuclear separation R, and the fraction $f_B(R)$ of alkali-metal–atom-noble-gas pairs which is bound at an internuclear separation R.

Pascale[18] are used. For Ne, the measurement of Ref. 19 of the potential curve for NaNe was used to estimate the curves for the other alkali-metal Ne molecules. Expressed in the Morse potential form

$$V(R)=D(e^{-2a(R-R_0)}-2e^{-a(R-R_0)}) . \quad (19)$$

The values $D=1.0$ meV and $a=0.89$ Å^{-1} were chosen to be the same for all the alkali-metal Ne pairs, and the equilibrium separations R_0 were chosen to be Na, 5.29 Å; K, 5.64 Å; Rb, 5.68 Å; and Cs, 5.80 Å. Potentials for alkali-metal–Rn molecules were extrapolated from alkali-metal–Xe and alkali-metal–Kr molecules. Here the values for the Morse potential were chosen to be $D=18$ meV and $a=0.8$ Å^{-1}, with the following values for R_0: Na, 5.1 Å; K, 5.3 Å; Rb, 5.4 Å; and Cs, 5.5 Å. The values for η used are the partial-wave (PW) results from Ref. 16: η(He)$=-5.3$, η(Ne)$=9.4$, η(Ar)$=-22$, η(Kr)$=44$, η(Xe)$=-73$, and η(Rn)$=114$.

Since the wave function ψ_0 is required at distances greater than the inner core of the alkali-metal atom, we have chosen to use the Coulomb wave functions of Bates and Damgaard.[20] These wave functions use the experimentally known binding energies to ensure the correct asymptotic behavior of the alkali-metal wave function. To obtain a better normalization, we have divided the Bates-Damgaard wave functions, as prescribed by Seaton,[21] by the factor $\sqrt{\rho}$, where $\rho=1+(2/\nu^3)d\mu/d\epsilon$, the binding energy of the valence electron in rydbergs is $-\epsilon$, the effective quantum number ν is defined by $\nu^2=-1/\epsilon$, and $\mu=n-\nu$ is the quantum defect of the orbital of principal quantum number n. From experimental data for the alkali-metal atoms Na, K, Rb, and Cs, respectively, we obtain for ν, 1.63, 1.77, 1.80, and 1.87, while for $d\mu/d\epsilon$ we obtain -0.066, -0.156, -0.209, and -0.284.

The precise form of the repulsive part of the van der Waals potential has a major effect on the evaluation of (18). For example, the potentials of Pascale and Vandeplanque, which were used to calculate the values of κ_0 in Table I give for RbKr at 100 °C, $\kappa_0/\eta^2=0.12$, if we use the potentials of Buck and Pauly,[22] the computed value of κ_0/η^2 is 0.089, a factor of 30% different.

The rate of change of κ_0 with temperature follows directly from (18) and is

$$\frac{d\kappa_0}{dT}=\frac{\eta^2}{kT^2}\int_0^\infty|\psi_0(R)|^2V(R)e^{-V(R)/kT}4\pi R^2dR . \quad (20)$$

We may define a temperature coefficient T_0 by

$$\frac{1}{T_0}=\frac{1}{\kappa_0}\frac{d\kappa_0}{dT} . \quad (21)$$

One can use the temperature coefficient T_0 to estimate the enhancement coefficient at a temperature T, different from the reference temperature T_r for which (18) and (20) were numerically evaluated, according to the formula

$$\kappa_0(T)=\left[1+\frac{T-T_r}{T_0}\right]\kappa_0(T_r) . \quad (22)$$

In Table III we list values of T_0 calculated with the same parameters used for Table I. For all of the noble gases except Rn, the temperature coefficients are large and positive, which means that the values of κ_0 will increase slightly with increasing temperature. Except for NaRn, all of the temperature coefficients for Rn are negative. The negative characteristic temperature means that κ_0 will decrease slightly with increasing temperature. This is because frequency-shift interactions at internuclear separations for the deep attractive well of the Rn A van der Waals potentials dominate over interactions on the repulsive inner barrier. The sign change in the temperature coefficient occurs for reasons closely analogous to the sign change with temperature of the Joule-Kelvin coefficient of gases.[23] The van der Waals potentials V and enhancement factors η are not known well enough to be sure about the predicted signs of T_0, that is, whether the enhancement factors κ_0 increase slightly or decrease slightly with temperature. The large magnitudes of T_0 implied by Table III are probably correct, that is, not much temperature dependence of κ_0 is to be expected for the heavier noble gases.

B. Frequency shifts at low pressures

In Eqs. (33) and (26) of Ref. 1 it was shown that bound van der Waals molecules shift the EPR frequency of alkali-metal atoms in the Zeeman multiplet of total angular momentum $f=I\pm\frac{1}{2}$ by

$$\delta\nu_f=\frac{1}{2\pi T_F}s(f,K)\langle K_z\rangle=\pm\frac{g_s\mu_B}{[I]h}(\delta B_A)_B , \quad (23)$$

where $1/T_F$ is the rate of formation of van der Waals molecules per alkali-metal atom and $\langle K_z\rangle$ is the mean longitudinal spin of the noble-gas nuclei. We have anticipated in the last term of (23) that it will be possible to describe the shift due to van der Waals molecules (denoted by the subscript B) with an effective magnitude field increment $(\delta B_A)_B$ of the form (16).

An approximate formula for the shift coefficient valid in the low-pressure, low magnetic field regime is given by Eq. (86) of Ref. 1 and is

$$s(f,K)=\pm\frac{\phi}{x[I]}\epsilon_{AX}=\pm\frac{\alpha\tau\epsilon_{AX}}{\hbar[I]} , \quad (24)$$

where the expression for the suppression factor ϵ_{AX} was already given by (8) in the introduction. Substituting (24), with α given by (1), into the middle of (23) and substituting (16) for δB_A into the right, with $\kappa_{AX}\rightarrow\epsilon_{AX}\kappa_1$ we find that the contribution to the field-enhancement factor of van der Waals molecules is

$$\epsilon_{AX}\kappa_1=\frac{|\psi|_B^2\tau\epsilon_{AX}}{T_F[X]}=k_{\text{chem}}|\psi|_B^2\epsilon_{AX} . \quad (25)$$

The chemical equilibrium constant for the van der Waals molecules k_{chem} has been introduced into (25) by means of the identity

$$k_{\text{chem}}=\frac{[XA]}{[X][A]}=\frac{\tau}{T_F[X]}=\frac{\tau}{T_K[A]} , \quad (26)$$

which holds in chemical equilibrium, between the mean breakup rate $1/\tau$ of the molecules and the mean molecular formation rate $1/T_F$ per alkali-metal atom, or the mean molecular formation rate $1/T_K$ per noble-gas atom. From classical statistical mechanics, the chemical equilibrium constant for the van der Waals molecules is

$$k_{\text{chem}}=\int_0^\infty f_B(R)e^{-V(R)/kT}4\pi R^2 dR \ , \tag{27}$$

where $f_B(R)$ is the probability that an alkali-metal-noble-gas pair at an internuclear separation R is in a bound or quasibound molecular state. We shall explain how $f_B(R)$ is determined in Sec. II C. For bound molecules, the average value of the valence-electron probability density $|\psi|_B^2$ at the site of the noble-gas nucleus is given by

$$\begin{aligned}\kappa_1&=\eta^2\int_0^\infty|\psi_0(R)|^2 f_B(R)e^{-V(R)/kT}4\pi R^2 dR\\&=k_{\text{chem}}|\psi|_B^2 \ .\end{aligned} \tag{28}$$

In Table II we have listed values of κ_1, calculated according to (28), with the same temperature, interatomic potentials and values of η that were used to calculate the values of κ_0 from (18).

The contribution of free alkali-metal–noble-gas pairs to the field-enhancement factor can be evaluated in analogy to (18) with the bound fraction f_B, which is taken into account by (28), excluded from the integral,

$$\begin{aligned}\kappa_0-\kappa_1=\eta^2\int_0^\infty|\psi_0(R)|^2[1-f_B(R)]\\ \times e^{-V(R)/kT}4\pi R^2 dR \ .\end{aligned} \tag{29}$$

The sum of (25) and (29) gives the total enhancement factor (4).

Similarly, in Eqs. (33) and (26) of Ref. 1 it was shown that bound van der Waals molecules shift the NMR frequency $\delta\nu_K$ of the noble-gas nuclei by an amount

$$\delta\nu_K=\frac{1}{2\pi T_K}\sum_f s(K,f)\langle f_z\rangle=-\frac{\mu_K}{Kh}(\delta B_X)_B \ , \tag{30}$$

where we have anticipated that the shift due to the van der Waals molecules can be written in terms of an effective magnetic field $(\delta B_X)_B$. Note that $\sum\langle f_z\rangle=\langle a_z\rangle+\langle b_z\rangle=\langle F_z\rangle=\langle S_z\rangle+\langle I_z\rangle$, where $\mathbf{F}=\mathbf{S}+\mathbf{I}$ is the total spin angular momentum operator of the alkali-metal atom. The frequency-shift coefficients are given by Eq. (87) of Ref. 1 and are

$$s(K,f)=\pm\frac{\phi}{x[I]}\epsilon_f=\pm\frac{\alpha\tau\epsilon_f}{[I]} \ , \tag{31}$$

where the suppression factors are

$$\begin{aligned}\epsilon_f=&\frac{2}{3}\frac{1}{1+(\phi/[I])^2}\\&+\frac{1}{f(f+1)[f]}\sum_{m_j=-f}^{f}\frac{(m_f)^2}{1+(\phi m_f/x[I])^2} \ .\end{aligned} \tag{32}$$

The suppression factor ϵ_a for the upper Zeeman multiplet $f=a=I+\frac{1}{2}$ of the alkali-metal atom, the suppression factor ϵ_b for the lower Zeeman multiplet $f=b=I-\frac{1}{2}$, computed according to (32), and the suppression factor ϵ_{XA} for the single Zeeman multiplet of the noble-gas atom, calculated according to (8), are sketched as a function $[I]/\phi$ in Fig. 2 for $^{85}Rb^{83}Kr$ with $x=9.85$ and $I=\frac{5}{2}$. We note that ϵ_{AX} differs significantly from ϵ_a and ϵ_b, but the latter two functions are both well represented by ϵ_{XA} which was defined by (9). For alkali-metal atoms with $I>\frac{1}{2}$ we will therefore make little error if we replace both ϵ_a and ϵ_b in (31) by ϵ_{XA} of (9). Then (30) becomes

$$\delta\nu_K=\frac{\alpha\tau\epsilon_{XA}}{hT_K}\left[\frac{\langle a_z\rangle-\langle b_z\rangle}{[I]}\right]=\frac{\alpha\tau\epsilon_{XA}}{hT_K}\langle S_z\rangle \ . \tag{33}$$

Substituting (33) into the left-hand side of (30), with α given by (1), and substituting (17) into the right-hand side, with $\kappa_{XA}\rightarrow\epsilon_{XA}\kappa_1$, we find that the contribution of van der Waals molecules to the enhancement factor must be

$$\epsilon_{XA}\kappa_1=k_{\text{chem}}|\psi|_B^2\epsilon_{XA} \tag{34}$$

in complete analogy to (25).

C. Determination of $f_B(R)$

The probability of finding an alkali-metal–noble-gas pair separated by R is proportional to

$$Z_0(R)=\int e^{-E/kT}d^3p=(2\pi\mu kT)^{3/2}e^{-V(R)/kT} \ , \tag{35}$$

where the integral extends over all momentum space for the relative motion of the pair and μ is the reduced mass. The energy is the sum of the van der Waals potential and the kinetic energy of the pair

$$E=V(R)+\frac{p^2}{2\mu} \ . \tag{36}$$

To calculate the bound fraction, we restrict the integral over momentum space to those momenta which correspond to bound states, and normalize to (35),

$$f_B(R)=\frac{1}{Z_0}\int_{\text{bound}}e^{-E/kT}d^3p \ . \tag{37}$$

For convenience, we write the energy as

$$E=V_N(R)+\frac{p_\parallel^2}{2\mu} \ , \tag{38}$$

where the effective potential energy is

$$V_N(R)=V(R)+\frac{(\hbar N)^2}{2\mu R^2} \ , \tag{39}$$

and $p_\parallel$ is the component of linear momentum along R. Representative values of $V_N(R)$ are shown in Fig. 3(a).

The rotational angular momentum of the molecule is related to the component of linear momentum $p_\perp$ transverse to the internuclear radius by

$$Rp_\perp=\hbar N \ . \tag{40}$$

Since the van der Waals potential is conservative and central and since the noncentral spin Hamiltonian (14) is relatively small and can only change N by one unit, the alkali-metal–noble-gas pair will oscillate along the effective potential V_N with essentially constant total energy E and rotational angular momentum N. The molecule will eventually be broken apart by collisions, or in the case of quasibound molecules with $E>0$ by spontaneous decay. As was already shown by Bouchiat *et al.*,[24] for pressures above a few tenths of a torr the spontaneous decay rates of most quasibound molecules are much smaller than the collisional breakup rates, and we will therefore ignore spontaneous decay of van der Waals molecules and the inverse process, resonant two-body molecular formation, in our subsequent discussion.

From inspection of Fig. 3 we see that molecules can exist only with angular momenta smaller than $N_c=102$ for the RbKr, where N_c is the angular momentum for which the local minimum of $V_N(R)$ becomes an inflection point. We define the function $E_{\max}(N)$ to be the maximum energy for which a state of angular momentum N can be bound. The maximum angular momentum $M(R)$ allowed for a bound molecule at internuclear separation R is found implicitly from the equation

$$E_{\max}(M)=V_M(R)\ . \tag{41}$$

If no bound states exist at R, we define $M(R)=0$.

With the above definitions, the fraction of bound molecules becomes

$$f_B(R)=\frac{\hbar^2}{Z_0R^2}\int_0^{M(R)}dN\,4\pi N e^{-V_N(R)/kT}\times\int_0^{p_{\parallel\max}}dp_\parallel e^{-p_\parallel^2/2\mu kT} \tag{42}$$

$$=\frac{\hbar^2}{\mu kTR^2}\int_0^{M(R)}dN\,N e^{-\hbar^2N^2/2\mu R^2kT}\times\mathrm{erf}(p_{\parallel\max}^2/2\mu kT)^{1/2}\ , \tag{43}$$

where $p_{\parallel\max}^2=2\mu[E_{\max}(N)-V_N(R)]$. A numerical calculation of $f_B(R)$ of RbKr is shown in Fig. 3(b). Note that it has a maximum of about 0.13 at the bottom of the van der Waals well.

For internuclear separations where the Boltzmann factor is on the order of 1 (i.e., except at the repulsive wall of the potential), the temperature dependence of $f_B(R)$ is dominated by the $T^{3/2}$ dependence of Z_0. Since the chemical equilibrium constant (27) and κ_1 involve integrals of $f_B(R)$ their temperature dependences will closely follow a $T^{-3/2}$ dependence. We have verified this by numerical calculations. For most molecules, the small size of κ_1 will make this temperature dependence unimportant.

III. EXPERIMENTAL STUDIES

We have performed experiments in which we have observed EPR frequency shifts in Rb-metal vapor due to polarized ^{83}Kr and ^{129}Xe, and NMR frequency shifts in ^{83}Kr and ^{129}Xe due to polarized Rb-metal vapor. A schematic of the experimental apparatus is shown in Fig. 4. The krypton studies were performed with a spherical pyrex glass cell containing 25 torr of krypton, isotopically enriched to 70% ^{83}Kr, and about 10 torr of nitrogen gas. The pressures are quoted for a cell filling temperature of 25 °C. The cell also contained several milligrams of rubidium metal of natural isotropic composition. The cell was contained in an oven, heated to a temperature of 90 °C by flowing hot air. This resulted in a Rb number density of about 3.0×10^{12} cm^{-3}.[2,25] A static magnetic field of about 0.1 G was produced by a solenoid, surrounded with two concentric μ-metal shields which reduce the field fluctuations to less than 1 mG. An optically pumped Cs magnetometer, not shown in Fig. 4, was located within 3 cm of the sample cell and was used to sense the total magnetic field. Any fluctuations in the field were canceled by feedback of current into the compensating coils of Fig. 4. The active stabilization held the longitudinal field at the cell constant to about 2 μG.

A key feature of this experiment was the detection of nuclear polarization by the observation of the induced EPR frequency shift in the rubidium. A feedback system was used to actively lock a voltage controlled oscillator (VCO) to the 90th harmonic of the EPR frequency ($\approx$51.28 kHz) of ^{85}Rb. The VCO output frequency was divided by a factor of 90, filtered, frequency modulated (FM) at 70 Hz, and applied to the Rb rf coils while the cell was probed by circularly polarized 7948-Å D_1 light from a Rb resonance lamp. The probe light, collected with a lens, was detected by a silicon photodiode, the output of which was fed to a lock-in amplifier. The 70-Hz modulation frequency of the rf provided the reference

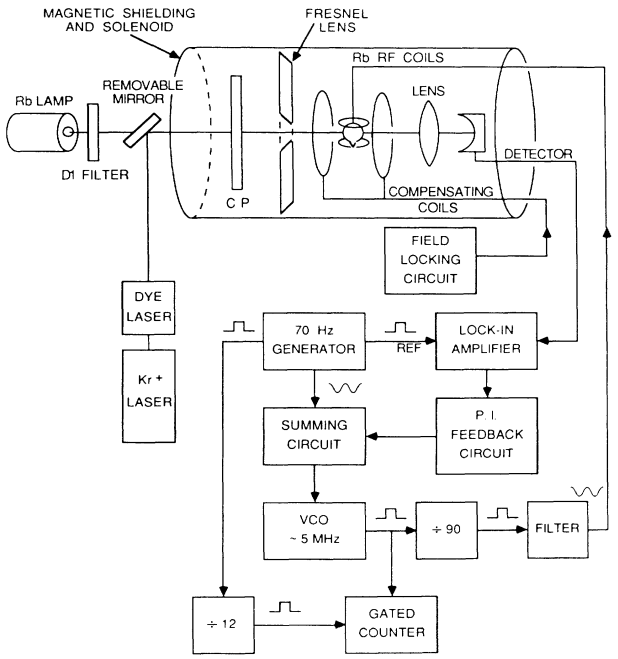

FIG. 4. Schematic diagram of the experimental apparatus. Only the frequency-locking apparatus is shown in detail. The important field-locking apparatus and the NMR coils are discussed in the text.

frequency for the lock-in amplifier. If we were to scan the central rf carrier frequency in an open-loop configuration, the output of the lock-in amplifier would resemble the derivative of the EPR resonance line. The lock-in thus provides a suitable error signal which can be processed through a feedback circuit containing both a proportional and an integral (P.I.) branch (shown in Fig. 4 as the P.I. feedback circuit), and can be applied to the control voltage of the VCO to keep its 90th subharmonic locked to the EPR resonance. The EPR frequency is determined by measuring the VCO frequency with a gated counter. The VCO frequency was chosen to be 90 times greater than the EPR frequency in order to reduce the measurement error during a specified gate time.

Each data point in the NMR lines of Fig. 1 was obtained using a technique that consisted of three distinct phases. In the first phase, the cell was subjected to a strong inhomogeneous oscillating magnetic field at the Larmor frequency of the krypton. This ensured that no polarization existed in the krypton. During the next phase, the Rb atoms in the vapor phase were maintained at high polarization by optically pumping with several hundred milliwatts of circularly polarized 7948-Å light from a cw dye laser, pumped by a krypton-ion laser. During this pumping phase, angular momentum was transferred from the spin-polarized Rb atoms to the nuclear spins of the ^{83}Kr atoms by spin-exchange collisions in van der Waals molecules.[1,2,10] Simultaneously, a homogeneous oscillating magnetic field was applied at the frequency specified in Fig. 1 as the NMR frequency. When the NMR frequency is near the Larmor frequency of the krypton atoms, the buildup of polarization is inhibited because of the precession of the krypton atoms. The final phase consists of probing the nuclear polarization of the krypton by measuring the EPR frequency shift in the Rb metal. During the pump phase, the polarization of the alkali-metal vapor can be oriented either parallel or antiparallel to the applied field, indicated by the circular and square data points, respectively. The splitting between the two NMR lines is thus twice the NMR frequency shift.

The line shape of resonance curves, such as those plotted in Fig. 1, are well understood when the energy of a magnetic sublevel of azimuthal quantum number m_K varies as $\hbar\omega_0 m_K$, as is the case when there is a pure magnetic dipole interaction with a homogeneous external field. In this case, the line shape is given by

$$\langle K_z \rangle = \langle K_z \rangle_{\max} \frac{(\Delta\omega)^2+\Gamma^2}{(\Delta\omega^2)+\Gamma^2+\Omega_1^2} , \tag{44}$$

where $\Delta\omega$ is the detuning of the oscillating magnetic field from the central frequency ω_0, Γ is the relaxation rate of the krypton polarization, and

$$\Omega_1 = \frac{1}{2\hbar}\frac{\mu_K}{K} H_1 , \tag{45}$$

where H_1 is the amplitude of the oscillating magnetic field. The factor of $\frac{1}{2}$ is needed because the oscillating field is composed of two rotating components. Only the component rotating in the same sense as the krypton precession has a significant effect.

The line shape for Fig. 1 is complicated by the existence of coherent quadrupole interaction[7] between the noble-gas nuclei and the walls of the slightly aspherical cell. Because of this, there are actually nine Zeeman intervals $\Delta E_n/\hbar \approx \omega_0 + n\Delta\omega_0$, where $-4 \le n \le 4$. We have measured $\Delta\omega_0$ in a manner similar to that for Ref. 7. The resulting spread in frequency of $8\Delta\omega_0/2\pi = 1.9 \pm 0.3$ mHz is approximately equal to the linewidth of the resonances shown in Fig. 1. For this reason, we have not used the known values of Γ and Ω_1 to fit the data, since the resulting lines are too narrow. Instead we allowed Γ and Ω_1 to vary from their known values in order to better fit the wings of the lines when determining line centers. It is this fit which is plotted in Fig. 1.

The Rb electron polarization in the cell $2\langle S_z \rangle$ determines the splittings between two resonance curves of Fig. 1. Care was taken to maintain the same optical pumping conditions for each of the data points. The actual polarization of the rubidium electrons, however, is not known to great accuracy. In a separate set of measurements, we measured the dependence of the ^{85}Rb EPR frequency shift on laser power, after pumping the cell long enough to allow the ^{83}Kr nuclear polarization to approach its saturation value. This is a direct indication of the volume-averaged rubidium hyperfine polarization $\langle F_z \rangle$. The measurements were compared to models of the optical pumping mechanisms in our system. These models included the effects of optical pumping, electron randomization, van der Waals molecular formation, diffusion, and refraction of the pumping light as it enters a spherical cell. Based on these models we infer that the rubidium electron polarization for the data of Fig. 1 was 45 ± 15 %.

This value of the rubidium polarization implies a value for κ_{KrRb} of 270 ± 95 at 90 °C. To arrive at our quoted error we have added in quadrature a 33% uncertainty in the rubidium electron polarization, a 10% uncertainty in the rubidium number density, and as much as a 5% error in other measured quantities. We note that we are confident of the rubidium number density at the 10% level because the cell was completely cured, that is, it had been maintained at a temperature of 90 °C for hundreds of hours, thus ensuring that the alkali-metal number density was no longer being effected by chemical reaction with the cell walls.

The ratio of the saturation value for $\Delta\nu_{\mathrm{EPR}}$ (51.1 ± 2.0 Hz for ^{85}Rb) to the value for $\Delta\nu_{\mathrm{NMR}}$ (4.9 ± 0.1 mHz) allows one to convert the rubidium frequency shift to an absolute polarization of the ^{83}Kr, as shown by the right-hand scale for Fig. 1. This scale is, however, subject to the 33% uncertainty from the value for the rubidium polarization. We estimate that the suppression factor was $\epsilon_{AX} \ge 0.95$ for the samples used in this experiment, which contained ≈ 25 torr of nitrogen gas. From inspection of Table II we conclude that the measured enhancement factors κ_{RbKr} and κ_{KrRb} of (2) and (3) were within 1% of the high-pressure limit κ_0. We have therefore entered our measurements as experimental determinations of κ_0 in Table IV.

In a similar experiment, we measured the frequency shifts of polarized ^{83}Kr and ^{129}Xe in a cell containing

both gases. The results of this measurement are summarized in Fig. 5. The observed EPR shifts were due to either the nuclear polarization of ^{83}Kr or the nuclear polarization of ^{129}Xe, but not to both. The relaxation times of the ^{83}Kr and ^{129}Xe in our cell were about 1000 and 60 s, respectively. When measuring the EPR shift due to ^{83}Kr, the data were taken 250 s after the laser was blocked. This assured that less than $1/(e^4)$ of the EPR shift was due to ^{129}Xe polarization. When measuring the EPR shift due to ^{129}Xe, two precautions were taken to ensure that the ^{83}Kr polarization was nearly zero. In addition to the oscillating field that was applied to scan the ^{129}Xe resonance, an oscillating magnetic field was also applied at the previously measured frequency of the ^{83}Kr resonance in order to inhibit the buildup of polarization. The rf power used was about five times higher than it had been while measuring the ^{83}Kr frequency shifts. The higher power caused the ^{83}Kr NMR line to be broadened, thus making small errors in the frequency less important. The second precaution was that a pump time of only three minutes was used. This allowed the ^{129}Xe to pump nearly to saturation, while the ^{83}Kr could at best reach about 17% of its saturation value. Since the oscillating field alone would inhibit at least 95% of the buildup of polarization, the reduced pumping period and the oscillating field together ensured that the ^{83}Kr contributed less than 1% of the measured EPR shift attributed to ^{129}Xe. During all of these measurements care was taken to keep the laser power constant, thus ensuring a nearly constant rubidium polarization.

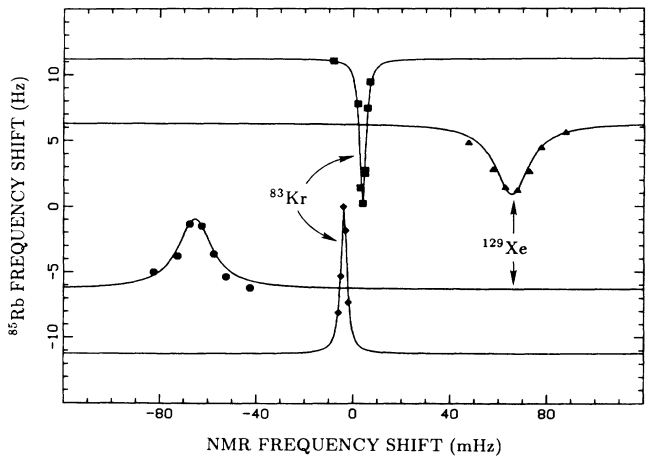

FIG. 5. Experimental determination of the NMR frequency shifts of ^{129}Xe and ^{83}Kr in the same sample cell. The lower two curves are for $\langle S_z \rangle$ and $\langle K_z \rangle$ parallel to the external magnetic field B, and the upper two curves are for $\langle S_z \rangle$ and $\langle K_z \rangle$ antiparallel to the external field. For a given alkali-metal atomic density [Rb] and electron-spin polarization $\langle S_z \rangle$, the ratio of the NMR frequency shift of ^{129}Xe to that of ^{83}Kr is 17.1±0.9. If the values of the alkali-metal number density (Rb) and the spin polarization $\langle S_z \rangle$ are constant, as they were in these measurements, the absolute values do not have to be known too precisely to determine the ratio of the enhancement factors $\kappa_{\mathrm{XeRb}}/\kappa_{\mathrm{KrRb}}=2.38\pm0.13$ from the ratio of the NMR frequency shifts.

According to (3), the ratio of the NMR frequency shifts should be given by

$$\frac{\Delta\nu_{\mathrm{Xe}}}{\Delta\nu_{\mathrm{Kr}}}=\frac{\kappa_{\mathrm{XeRb}}\mu_{\mathrm{Xe}}K_{\mathrm{Kr}}}{\kappa_{\mathrm{KrRb}}\mu_{\mathrm{Kr}}K_{\mathrm{Xe}}}\ , \tag{46}$$

which is independent of alkali-metal number density and polarization. Thus, the ratio is independent of the major sources of systematic error present in the individual frequency-shift measurements. The gas pressures, about 0.2 torr for ^{129}Xe and 20 torr for ^{83}Kr, were chosen so that the ^{85}Rb frequency shifts due to the two gases were approximately equal. Substituting our measured ratio 17.1±0.9 and the known values of the nuclear spins ($K_{\mathrm{Xe}}=\frac{1}{2}$ for ^{129}Xe and $K_{\mathrm{Kr}}=\frac{9}{2}$ for ^{83}Kr) and moments (in nuclear magnetons, $\mu_{\mathrm{Xe}}=-0.772$ for ^{129}Xe and $\mu_{\mathrm{Kr}}=-0.967$ for ^{83}Kr) into (46) we find

$$\frac{\kappa_{\mathrm{XeRb}}}{\kappa_{\mathrm{KrRb}}}=2.38\pm0.13\ . \tag{47}$$

Combining this with our direct measurement $\kappa_{\mathrm{KrRb}}=270\pm95$ implies that $\kappa_{\mathrm{XeRb}}=643\pm260$.

Although we have not measured the pressure dependence of κ_{AX} or κ_{XA} to obtain values for κ_1, we can deduce κ_1 from other measurements and so estimate the molecular contributions to the frequency shifts. We find from (25) and (1)

$$\kappa_1=\frac{k_{\mathrm{chem}}\alpha}{(8\pi/3)g_S\mu_B(\mu_K/K)}\ . \tag{48}$$

Substituting into (26) values of τ and T_F inferred from the measurements of τp and $T_F p^2$ of Bouchiat *et al.*,[26] and noting that $p=[X]kT$ for their work, we find that the chemical equilibrium constant of RbKr is $k_{\mathrm{chem}}=(1.52\pm0.12)\times10^{-22}$ cm^3. Combining the measured spin-rotation constant $\gamma N/h=26.8\pm0.8$ MHz from Bouchiat *et al.*[26] with the measurement of $x=\gamma N/\alpha=9.85\pm1.97$ by Schaefer,[27] we find $\alpha/h=2.72\pm0.54$ MHz for RbKr. Substituting these experimental values into (48) gives $\kappa_1=16.2\pm3.5$ at 300 K. In a similar way the measurements of Zeng *et al.*[2] and Bouchiat *et al.*[26] were used to infer the experimental values for κ_1, which are entered into Table IV for KXe, RbXe, and CsXe.

IV. CONCLUSIONS

The results of this paper show that the NMR and EPR frequency shifts which are observed in mixtures of nuclear-spin-polarized noble gases and vapors of spin-polarized alkali-metal atoms can be quantitatively described by the Fermi-contact interaction $\alpha\mathbf{K}\cdot\mathbf{S}$ between the nuclear spin $\mathbf{K}$ of the noble-gas atom and the valence-electron spin $\mathbf{S}$ of the alkali-metal atom. Some of the most important conclusions of this work are as follows.

(1) The high ($\approx$50%) electron-spin polarizations of the alkali-metal atoms in these experiments produced NMR frequency shifts which substantially exceeded the width of the NMR lines (see Figs. 1 and 5).

(2) The low ($\leq 5\%$) nuclear-spin polarizations of the noble-gas atoms in these experiments produced EPR frequency shifts which were only about 5% of the EPR linewidth.

(3) Both NMR and EPR frequency shifts can be measured with great precision with the actively field-locked and frequency-locked apparatus of Sec. III.

(4) For quantitative comparisons between experiment and theory, the most difficult experimental parameters to measure are the spin polarizations $\langle K_z \rangle$ and $\langle S_z \rangle$. The alkali-metal atom number density can also be subject to large uncertainties if it is inferred from saturated vapor curves and sample temperatures. It is common experience that the alkali-metal vapor pressures can be substantially smaller than expected because of chemical reactions at the cell walls. Measurements of ratios of frequency shifts in the same cell often avoid these problems.

(5) The agreement between the measured and predicted values of the enhancement factors, summarized in Table IV, is fairly good. Initial estimates for the enhancement factors for other alkali-metal-atom–noble-gas pairs can therefore be obtained with some confidence from the predicted values of Tables I through III.

(6) The theoretically predicted frequency shifts are almost totally due to binary collisions in the lighter noble gases, and even for a gas as heavy as radon, the contribution of van der Waals molecules to the frequency shifts is probably no more than 15%. In contrast, the spin-exchange rates and spin-relaxation rates for the heavier noble gases are dominated by contributions from van der Waals molecules, except at very high sample pressures.

(7) According to theory, the contributions of van der Waals molecules to the frequency shifts are suppressed by a factor ϵ at low pressures. Formula for ϵ are given by (8) and (9).

(8) The reliability of the theoretical computations of the frequency shifts is limited by poorly known van der Waals potentials V and by equally poorly known enhancement factors η for valence-electron wave functions at the nuclei of noble gases. Precise experimental measurements of the shifts could serve as an excellent constraint on V and η, and could lead to much more precisely determined values of both.

(9) Measurements of the EPR frequency shift caused by polarized noble gas in spin-polarized targets could be a precise and convenient way to determine absolute nuclear polarizations if careful measurements were made of κ_0. For both He and Ne, theory (see Table II) indicates that the pressure-dependent contributions to the frequency shifts should be completely negligible, but that it would be important to account for possible cell-geometry-dependent contributions to the shift due to long-range magnetic dipole-dipole interactions. In the cases of Kr and Xe, however, the geometry dependence of the shift should be less than 1%, and at pressures greater than about 100 torr, the pressure dependence of the shift should be at worst several percent.

ACKNOWLEDGMENTS

We gratefully acknowledge discussions with our colleagues at Princeton University. This work was supported by the U.S. Air Force Office of Scientific Research, under Grant No. 88-0165.

[1]W. Happer, E. Miron, S. Schaefer, D. Schreiber, W. A. van Wijngaarden, and X. Zeng, Phys. Rev. A **29**, 3092 (1984).
[2]X. Zeng, Z. Wu, T. Call, E. Miron, D. Schreiber, and W. Happer, Phys. Rev. A **31**, 260 (1985).
[3]F. P. Calaprice, W. Happer, D. F. Schreiber, M. M. Lowry, E. Miron, and X. Zeng, Phys. Rev. Lett. **54**, 174 (1985).
[4]M. Kitano, M. Bourzutschky, F. P. Calaprice, J. Clayhold, W. Happer, and M. Musolf, Phys. Rev. A **34**, 1974 (1986).
[5]M. Kitano, F. P. Calaprice, M. L. Pitt, J. Clayhold, W. Happer, M. Kadar-Kallen, M. Musolf, G. Ulm, T. Chupp, J. Bonn, R. Neugart, E. Otten, and H. T. Duong, Phys. Rev. Lett. **60**, 2133 (1988).
[6]T. G. Vold, F. Raab, B. Heckel, and E. N. Fortson, Phys. Rev. Lett. **52**, 2229 (1984).
[7]Z. Wu, S. Schaefer, G. D. Cates, and W. Happer, Phys. Rev. A **37**, 1161 (1988).
[8]Z. Wu, W. Happer, and J. M. Daniels, Phys. Rev. Lett. **59**, 1480 (1987).
[9]T. E. Chupp, M. E. Wagshul, K. P. Coulter, A. B. McDonald, and W. Happer, Phys. Rev. C **36**, 2244 (1987).
[10]B. C. Grover, Phys. Rev. Lett. **40**, 391 (1978).
[11]W. D. Knight, Solid State Phys. **2**, 93 (1950).
[12]M. Arditi and T. R. Carver, Phys. Rev. **112**, 449 (1958); F. J. Adrian, J. Chem. Phys. **127**, 837 (1960).
[13]Julia Hsu, Z. Wu, and W. Happer, Phys. Lett. **112A**, 141 (1985).
[14]R. M. Herman, Phys. Rev. **137**, A1062 (1965).
[15]Charles Kittel, *Introduction to Solid State Physics* (Wiley, New York, 1967), p. 378.
[16]T. G. Walker, K. Bonin, and W. Happer, Phys. Rev. A **35**, 3749 (1987).
[17]J. Pascale and J. Vandeplanque, J. Chem. Phys. **60**, 2278 (1974).
[18]J. Pascale, Phys. Rev. A **28**, 632 (1983).
[19]W. P. Lapadovitch, R. Ahmad-Bitar, P. E. Moskowitz, I. Renhorn, R. Gottscho, and D. E. Pritchard, J. Chem. Phys. **73**, 5419 (1980).
[20]D. R. Bates and A. Damgaard, Philos. Trans. R. Soc. London **242**, 101 (1949).
[21]M. J. Seaton, Mon. Not. R. Astron. Soc. **188**, 504 (1969).
[22]U. Buck and H. Pauly, Z. Phys. **208**, 390 (1968).
[23]L. D. Landau and E. M. Lifshitz, *Statistical Physics* (Pergamon, London, 1958), p. 223.
[24]C. C. Bouchiat, M. A. Bouchiat, and L. C. L. Pottier, Phys. Rev. **181**, 144 (1969).
[25]T. Killian, Phys. Rev. **27**, 578 (1926).
[26]M. A. Bouchiat, J. Brossel, and L. C. L. Pottier, J. Chem. Phys. **56**, 3703 (1972).
[27]S. R. Schaefer, Ph.D. thesis, Princeton University, 1988 (unpublished).